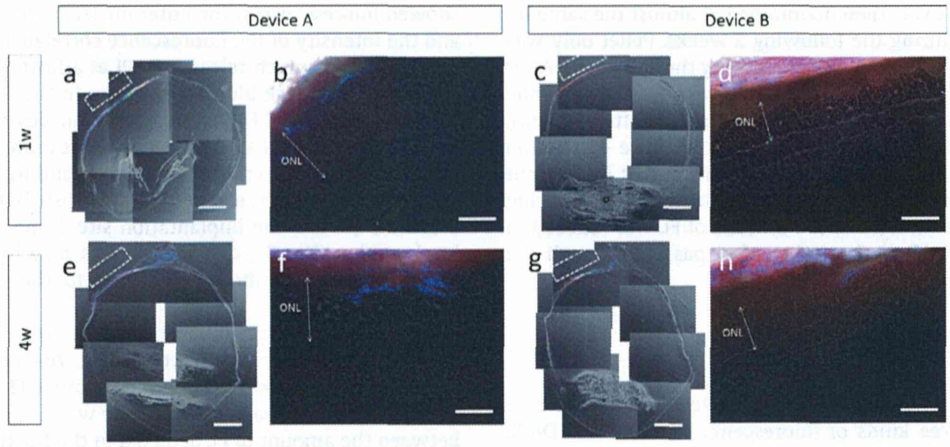

Fig. 6. (a–h) The distribution of FL (green), Rho (red) and DAPI (blue) in the retina and sclera around the implantation site 1 week (a–d) and 4 weeks (e–h) after implantation (square dots: device implantation site). Two types of devices, device A (F60/R40/D60) and B (F60/R60/D40), were used. Device A shows faster DAPI release than Rho and device B shows faster Rho release than DAPI. Magnified images (b, d, f, h) show that fluorescents reached the outer nuclear layer (ONL, double-headed allows). Scale bars, 1 mm (a, c, e, g) and 100 μm (b, d, f, h).

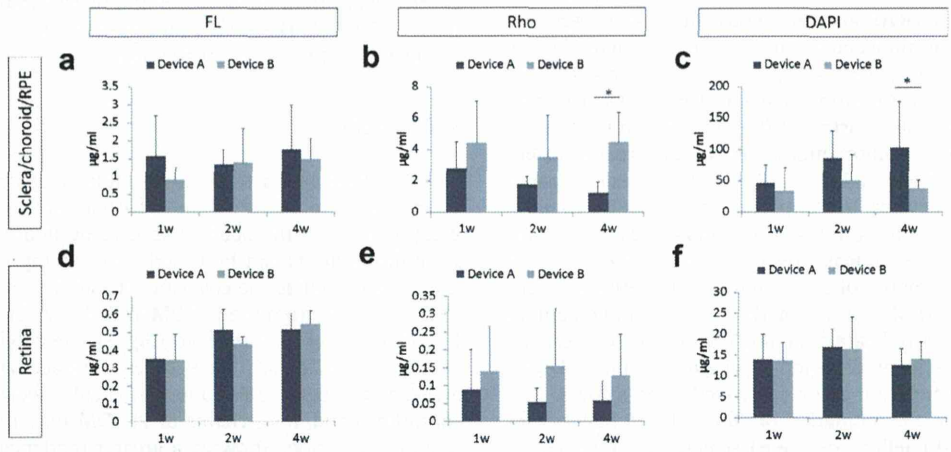

Fig. 7. The amounts of FL, Rho and DAPI in the sclera/choroid/RPE (a–c) and retinal fractions (d–f) during 4 weeks' implantation. Values are mean ± SD. $^{*}p < 0.05$ (unpaired *t*-test for normally distributed isolated pairs).

conditions (Supplementary Fig. S.2), indicating that the permeability may be influenced by the physical characteristics of the substance, such as lipophilicity, water solubility and acid–base character; FL and Rho-B are weak carboxylic acids, while DAPI is a base [33]. Therefore, we need to consider the physical characteristics of the substances and their interactions when determining the optimum PEGDM/TEGDM system for the intended drug release.

The device materials, PEGDM and TEGDM, are bio-inert and can be easily molded into different substrate shapes by UV curing [34,35]. We used a microfabrication technique because the shape and volume of the reservoir can be easily modified by an AutoCAD design. We have previously reported a reservoir-based protein-drug-release device sealed with a PEGDM cover including collagen microparticles, which served as permeation porogen for macromolecules [36]. We found that low-molecular-weight molecules can easily pass through polymerized PEGDM membrane, whereas polymerized TEGDM is impermeable to them (Fig. 2). Therefore, we newly developed a controlled release system for low-molecular-weight drugs using a PEGDM/TEGDM mixture. Some monomers of unpolymerized PEGDM and TEGDM and photoinitiator were found to elute from the device, but the amount of elution (the highest amount is 504 ng ml^{-1}) was significantly less than cytotoxically active levels (more than 391 μg ml^{-1}), and no more monomers and photoinitiator eluted after incubation in PBS for 15 days (Supplementary Fig. S.4). The PEGDM/TEGDM polymer shows almost no biodegradation 19 months after implantation on the rabbit sclera (Supplementary Fig. S.5). Additionally, the long-term implantation of the device over 4 weeks did not affect retinal function assessed by electroretinograms (Supplementary Fig. S.6). Thus, the device would appear to be stable and biocompatible for at least 1 year, and can be used to safely administer drugs by the transscleral approach without disturbing intraocular tissues.

Fluorescents were used for the analysis of drug transport into the eye from the device. Although fluorescence was observable in the ocular tissues during 4 weeks' implantation and distributed locally around the implantation site, the fluorescein concentration in the retina seemed to be almost the same in spite of the difference in the release profiles of the devices (Figs. 4f and 7e and f). This may be due to the blood–retinal barrier restricting drug transport through the RPE to the retina. Pitkanen reported that the permeability through the RPE depended on the lipophilicity and molecular weight of drugs [37]. Additionally, transporters in the RPE probably have a greater role in ocular pharmacokinetics [38]. In

fact, we observed FL accumulation around the RPE (Fig. 4d), indicating that the drug transport was restricted here. This may be one of the reasons for the constant amount of fluorescents in the retina. Additionally, this behavior might be due to the availability of fluorescents at the retina, because transport and penetration through the sclera, choroid and RPE may vary between molecules [37]. The clearance rate by blood vessels may also be different for hydrophobic and hydrophilic molecules [15]. Our device has a low-molecular-weight-impermeable reservoir that can release drugs unidirectionally to the sclera, making it less susceptible to drug elimination by conjunctival lymphatic/blood vessel clearance, so the choroid may be the primary route of clearance. Further study is needed to elucidate the factors influencing drug availability to the retina. Given that the distribution of fluorescents was concentrated at the RPE and adjacent regions, our device may be effective, especially for lesions in the vicinity of the RPE.

One of the limitations of this study is the lack of a study proving retinal neuroprotective effects of our device using clinical drugs. Previous reports show potent effective drugs, such as edaravone [39], geranylgeranylaceton [40] and unoprostone [41] against retinal degeneration in animals, whereas these drugs are administered via systemic route, topical eye drop or intravitreal injection. We are planning to perform an animal study using the clinical drugs to investigate the efficacy of our controlled transscleral multi-drug delivery system on retinal neuroprotection.

5. Conclusion

A polymeric system which can administer multiple compounds with distinct kinetics to the posterior segment of the eye was manufactured. The release of multiple compounds can be tuned by changing their formulations as well as the device covering. Furthermore, our system can be used to safely administer drugs by the transscleral approach without disturbing intraocular tissues. Strict local delivery of the drugs through our device may facilitate the administration of the drugs that would not be suitable for systemic use due to side-effects. Additionally, prolonged sustained drug release using our device would be suitable for the treatment of chronic retinal diseases. Thus, our polymeric system provides prolonged action and less invasive intraocular administration, and is expected to provide new tools for the treatment of posterior eye diseases with new therapeutic modalities.

Competing financial interests

The authors declare no conflict of interest.

Acknowledgements

This study was supported by Grant-in-Aid for Young Scientists (A) from the Ministry of Education, Culture, Sports, Science, and Technology 23680054 (N.N.), Health Labour Sciences Research Grant from the Ministry of Health Labour and Welfare H23-iryokiki-wakate-003 (N.N.), H23-kankaku-ippan-004 (T.A. and N.N.), H24-nanchitoh-ippan-067 (T.A. and N.N.), the Takeda Science Foundation (N.N.), the Tohoku University Exploratory Research Program for Young Scientists (N.N.) and Gonryo Medical Foundation (N.N.). We thank T. Kawashima, N. Kumasaka, T. Yamada and S. Ito for help with device molds preparation.

Appendix A. Supplementary data

Supplementary data associated with this article can be found, in the online version, at http://dx.doi.org/10.1016/j.actbio.2013.11.004.

References

[1] Resnikoff S, Pascolini D, Etya'ale D, Kocur I, Pararajasegaram R, Pokharel GP, et al. Global data on visual impairment in the year 2002. Bull World Health Organ 2004;82:844–51.
[2] Gragoudas ES, Adamis AP, Cunningham Jr ET, Feinsod M, Guyer DR. Pegaptanib for neovascular age-related macular degeneration. N Engl J Med 2004;351:2805–16.
[3] Kim M, Yoon BJ. Adaptive reference update (ARU) algorithm. A stochastic search algorithm for efficient optimization of multi-drug cocktails. BMC Genomics 2012;13(Suppl 6):S12.
[4] Calkins DJ. Critical pathogenic events underlying progression of neurodegeneration in glaucoma. Prog Retin Eye Res 2012;31:702–19.
[5] Fu QL, Li X, Yip HK, Shao Z, Wu W, Mi S, et al. Combined effect of brain-derived neurotrophic factor and LINGO-1 fusion protein on long-term survival of retinal ganglion cells in chronic glaucoma. Neuroscience 2009;162:375–82.
[6] Shin DH, Feldman RM, Sheu WP. Efficacy and safety of the fixed combinations latanoprost/timolol versus dorzolamide/timolol in patients with elevated intraocular pressure. Ophthalmology 2004;111:276–82.
[7] Spaide RF. Rationale for combination therapy in age-related macular degeneration. Retina 2009;29:S5–7.
[8] He S, Xia T, Wang H, Wei L, Luo X, Li X. Multiple release of polyplexes of plasmids VEGF and bFGF from electrospun fibrous scaffolds towards regeneration of mature blood vessels. Acta Biomater 2012;8:2659–69.
[9] Campochiaro PA. Potential applications for RNAi to probe pathogenesis and develop new treatments for ocular disorders. Gene Ther 2006;13:559–62.
[10] Frasson M, Picaud S, Leveillard T, Simonutti M, Mohand-Said S, Dreyfus H, et al. Glial cell line-derived neurotrophic factor induces histologic and functional protection of rod photoreceptors in the rd/rd mouse. Invest Ophthalmol Vis Sci 1999;40:2724–34.
[11] Rosenfeld PJ, Brown DM, Heier JS, Boyer DS, Kaiser PK, Chung CY, et al. Ranibizumab for neovascular age-related macular degeneration. N Engl J Med 2006;355:1419–31.
[12] Hughes PM, Olejnik O, Chang-Lin JE, Wilson CG. Topical and systemic drug delivery to the posterior segments. Adv Drug Deliv Rev 2005;57:2010–32.
[13] Del Amo EM, Urtti A. Current and future ophthalmic drug delivery systems. A shift to the posterior segment. Drug Discov Today 2008;13:135–43.
[14] Geroski DH, Edelhauser HF. Transscleral drug delivery for posterior segment disease. Adv Drug Deliv Rev 2001;52:37–48.
[15] Ranta VP, Urtti A. Transscleral drug delivery to the posterior eye: prospects of pharmacokinetic modeling. Adv Drug Deliv Rev 2006;58:1164–81.
[16] Ambati J, Adamis AP. Transscleral drug delivery to the retina and choroid. Prog Retin Eye Res 2002;21:145–51.
[17] Olsen TW, Edelhauser HF, Lim JI, Geroski DH. Human scleral permeability. Effects of age, cryotherapy, transscleral diode laser, and surgical thinning. Invest Ophthalmol Vis Sci 1995;36:1893–903.
[18] Li X, Zhang Z, Li J, Sun S, Weng Y, Chen H. Diclofenac/biodegradable polymer micelles for ocular applications. Nanoscale 2012;4:4667–73.
[19] Patel SR, Berezovsky DE, McCarey BE, Zarnitsyn V, Edelhauser HF, Prausnitz MR. Targeted administration into the suprachoroidal space using a microneedle for drug delivery to the posterior segment of the eye. Invest Ophthalmol Vis Sci 2012;53:4433–41.
[20] Aksungur P, Demirbilek M, Denkbas EB, Vandervoort J, Ludwig A, Unlu N. Development and characterization of Cyclosporine A loaded nanoparticles for ocular drug delivery: cellular toxicity, uptake, and kinetic studies. J Control Release 2011;151:286–94.
[21] Chhablani J, Nieto A, Hou H, Wu EC, Freeman WR, Sailor MJ, et al. Oxidized porous silicon particles covalently grafted with daunorubicin as a sustained intraocular drug delivery system. Invest Ophthalmol Vis Sci 2013;54:1268–79.
[22] Chen CW, Lu DW, Yeh MK, Shiau CY, Chiang CH. Novel RGD-lipid conjugate-modified liposomes for enhancing siRNA delivery in human retinal pigment epithelial cells. Int J Nanomedicine 2011;6:2567–80.
[23] Kaiser JM, Imai H, Haakenson JK, Brucklacher RM, Fox TE, Shanmugavelandy SS, et al. Nanoliposomal minocycline for ocular drug delivery. Nanomedicine 2013;9:130–40.
[24] Li X, Zhang Z, Chen H. Development and evaluation of fast forming nano-composite hydrogel for ocular delivery of diclofenac. Int J Pharm 2013;448:96–100.
[25] Wang CH, Hwang YS, Chiang PR, Shen CR, Hong WH, Hsiue GH. Extended release of bevacizumab by thermosensitive biodegradable and biocompatible hydrogel. Biomacromolecules 2012;13:40–8.
[26] Kunou N, Ogura Y, Yasukawa T, Kimura H, Miyamoto H, Honda Y, et al. Long-term sustained release of ganciclovir from biodegradable scleral implant for the treatment of cytomegalovirus retinitis. J Control Release 2000;68:263–71.
[27] Zhang H, Zhao C, Cao H, Wang G, Song L, Niu G, et al. Hyperbranched poly(amine-ester) based hydrogels for controlled multi-drug release in combination chemotherapy. Biomaterials 2010;31:5445–54.
[28] Shin HC, Alani AW, Rao DA, Rockich NC, Kwon GS. Multi-drug loaded polymeric micelles for simultaneous delivery of poorly soluble anticancer drugs. J Control Release 2009;140:294–300.
[29] Richardson TP, Peters MC, Ennett AB, Mooney DJ. Polymeric system for dual growth factor delivery. Nat Biotechnol 2001;19:1029–34.
[30] Lammers T, Subr V, Ulbrich K, Peschke P, Huber PE, Hennink WE, et al. Simultaneous delivery of doxorubicin and gemcitabine to tumors in vivo using prototypic polymeric drug carriers. Biomaterials 2009;30:3466–75.

[31] Elia R, Fuegy PW, VanDelden A, Firpo MA, Prestwich GD, Peattie RA. Stimulation of in vivo angiogenesis by in situ crosslinked, dual growth factor-loaded, glycosaminoglycan hydrogels. Biomaterials 2010;31:4630–8.
[32] Wang Y, Wang B, Qiao W, Yin T. A novel controlled release drug delivery system for multiple drugs based on electrospun nanofibers containing nanoparticles. J Pharm Sci 2010;99:4805–11.
[33] Dickens SH, Flaim GM, Floyd CJ. Effects of adhesive, base and diluent monomers on water sorption and conversion of experimental resins. Dent Mater 2010;26:675–81.
[34] Benoit DS, Durney AR, Anseth KS. Manipulations in hydrogel degradation behavior enhance osteoblast function and mineralized tissue formation. Tissue Eng 2006;12:1663–73.
[35] Kalachandra S. Influence of fillers on the water sorption of composites. Dent Mater 1989;5:283–8.
[36] Kawashima T, Nagai N, Kaji H, Kumasaka N, Onami H, Ishikawa Y, et al. A scalable controlled-release device for transscleral drug delivery to the retina. Biomaterials 2011;32:1950–6.
[37] Pitkanen L, Ranta VP, Moilanen H, Urtti A. Permeability of retinal pigment epithelium: effects of permeant molecular weight and lipophilicity. Invest Ophthalmol Vis Sci 2005;46:641–6.
[38] Mannermaa E, Vellonen KS, Urtti A. Drug transport in corneal epithelium and blood-retina barrier: emerging role of transporters in ocular pharmacokinetics. Adv Drug Deliv Rev 2006;58:1136–63.
[39] Imai S, Inokuchi Y, Nakamura S, Tsuruma K, Shimazawa M, Hara H. Systemic administration of a free radical scavenger, edaravone, protects against light-induced photoreceptor degeneration in the mouse retina. Eur J Pharmacol 2010;642:77–85.
[40] Tanito M, Kwon YW, Kondo N, Bai J, Masutani H, Nakamura H, et al. Cytoprotective effects of geranylgeranylacetone against retinal photooxidative damage. J Neurosci 2005;25:2396–404.
[41] Tsuruma K, Tanaka Y, Shimazawa M, Mashima Y, Hara H. Unoprostone reduces oxidative stress- and light-induced retinal cell death, and phagocytotic dysfunction, by activating BK channels. Mol Vis 2011;17:3556–65.

ADVANCED MATERIALS
www.advmat.de

Micropatterned Polymeric Nanosheets for Local Delivery of an Engineered Epithelial Monolayer

Toshinori Fujie, Yoshihiro Mori, Shuntaro Ito, Matsuhiko Nishizawa, Hojae Bae, Nobuhiro Nagai, Hideyuki Onami, Toshiaki Abe, Ali Khademhosseini, and Hirokazu Kaji**

Age-related macular degeneration (AMD) is a major ophthalmic disease that causes visual impairment and blindness, particularly in elderly people.[1] The pathogenesis of AMD is believed to result from the development of subretinal choroidal neovascularization triggered by an increment in secretion of vascular endothelial growth factor from retinal pigment epithelial (RPE) cells. The developing choroidal vessels invade Bruch's membrane and disrupt the RPE monolayer. Subsequently, degeneration of photoreceptors occurs and results in permanent visual loss. Hence, subretinal transplantation of RPE cells to the site of degeneration would offer an ideal treatment providing the transplanted cells could generate a monolayer, reconstruct the RPE–photoreceptor interface, and inhibit further development of choroidal vessels. Although transplantation of autologous peripheral RPE cells has been tested by injection of cell suspensions using a syringe, limited visual improvement result due to the low viability of the injected cells, and their restricted distribution and integration into the subretinal tissue.[2] In fact, we previously reported the transplantation of epithelial cells into animal models of AMD and found that similar problems to those described above occurred in the animals and that these difficulties held back further experimental development of potential therapeutic treatments.[3]

As a consequence of these problems, tissue engineering is expected to provide innovative therapeutics in regenerative medicine by directing cellular organization using microfabrication techniques.[4] Efforts are in progress towards an alternative approach which involves the local delivery of an engineered RPE monolayer using biocompatible devices. There have been several reports on the development of natural and synthetic substrates for cell delivery using collagen, poly(ethylene terephthalate) and poly(methyl methacrylate).[5] However, these engineered substrates are typically micrometers in thickness (6 μm at thinnest) and several millimeters in size. Therefore, they are not sufficiently flexible to be aspirated and injected through a conventional syringe needle into the narrow subretinal space. Thus, a large incision of the sclera and retinal tissue would be required for the injection of these rigid substrates, which would also require use of a custom-made metallic cannula with a millimeter-size rectangular opening.[5c] However, such an incision might result in leakage of vitreous fluid and lead to post-surgical infection. To minimize damage to host tissues and at the same time transplant an RPE monolayer that can withstand the required surgical manipulation, the substrates need to be simultaneously robust, extremely flexible and compliant in narrow spaces. Therefore, miniaturization of the substrates (for both thickness and size) is an important approach to achieve minimally invasive delivery of the engineered RPE monolayer.

Ultrathin polymeric films (nanosheets) are a relatively new class of soft nanomaterials that are under study in the polymer physics field.[6] Polymeric nanosheets range from tens to hundreds of nanometers thick with a very large aspect ratio (greater than 10^6) and, unlike bulk polymeric films, have unique physical properties. Their thermodynamic and mechanical properties vary in a thickness-dependent manner, resulting in high flexibility, non-covalent adhesiveness, and selective molecular permeability.[7] These properties are beneficial for biomedical applications, such as wound dressings and cellular scaffolds.[8] Previously, we demonstrated that the large surface area of

Y. Mori, S. Ito, Prof. M. Nishizawa, Prof. H. Kaji
Department of Bioengineering and Robotics
Graduate School of Engineering
Tohoku University
6–6–01 Aramaki, Aoba-ku, Sendai 980–8579, Japan
E-mail: kaji@biomems.mech.tohoku.ac.jp
Dr. T. Fujie, Prof. A. Khademhosseini
WPI-Advanced Institute for Materials Research (WPI-AIMR)
Tohoku University
2–1–1 Katahira, Aoba-ku, Sendai 980–8577, Japan
E-mail: alik@rics.bwh.harvard.edu
Prof. A. Khademhosseini
Center for Biomedical Engineering
Department of Medicine
Brigham and Women's Hospital
Harvard Medical School
Harvard-MIT Division of Health Sciences and Technology
Massachusetts Institute of Technology
Wyss Institute for Biologically Inspired Engineering
Harvard University
PRB-252, 65 Landsdowne Street, Cambridge, MA 02139, USA
Dr. T. Fujie
Department of Life Science and Medical Bioscience
School of Advanced Science and Engineering
Waseda University
TWIns, 2-2 Wakamatsu-cho, Shinjuku-ku Tokyo 162-8480, Japan
Prof. H. Bae
College of Animal Bioscience and Technology
Department of Bioindustrial Technologies
Konkuk University
Hwayang-dong, Kwangjin-gu, Seoul 143–701, Republic of Korea
Dr. N. Nagai, Dr. H. Onami, Prof. T. Abe
Division of Clinical Cell Therapy
United Centers for Advanced Research
and Translational Medicine (ART)
Tohoku University Graduate School of Medicine
2–1 Seiryo, Aoba-ku, Sendai 980–8575, Japan

DOI: 10.1002/adma.201304183

ADVANCED MATERIALS
www.advmat.de

Materials Views
www.MaterialsViews.com

polymeric nanosheets was of value for creating flexible substrates with thickness-dependent mechanical properties; these substrates could provide an adhesion interface for cardiomyocytes in a stiffness-dependent manner or could assist in the engineering of biomimetic structures.[9] Recently, we also showed that the surface property could be tailored by integration of nanoparticles or nanotubes,[10] which enhanced the morphological guidance of the skeletal muscle cells.[10b] Thus, we hypothesized that polymeric nanosheets would be an ideal platform to culture RPE cells, on which an engineered RPE monolayer is capable of withstanding deformation within a syringe needle, of recovering their original shape in the subretinal space, and of attaching to the lesion.

Here, we developed micropatterned nanosheets that supported the growth of an RPE cell line (RPE-J cells) and enabled the transplantation of the cells through a syringe needle without loss of cell viability. The micropatterned nanosheets consisted of biodegradable poly(lactic-*co*-glycolic acid) (PLGA), on which a monolayer of RPE-J cells formed. In addition, we embedded magnetic nanoparticles (MNPs, 10 nm ϕ) into the structure to improve optical visualization, manipulability, and cell morphogenesis. The viability of RPE-J cells on the micropatterned nanosheets was evaluated following the syringe manipulation step for transplantation of the engineered RPE monolayer. We also demonstrated the subretinal injectability of micropatterned nanosheets, their handling properties, and their physical stability using a swine eye model. To our knowledge, this is the first report of the development of an ultrathin flexible carrier that has the promise of minimally invasive delivery of a cellular organization into narrow tissue spaces.

Micropatterned nanosheets were prepared on poly(vinyl alcohol) (PVA)-coated substrates by a combination of a spincoating and microcontact printing technique using poly(dimethyl siloxane) (PDMS) molds (see Figure S1 in the Supporting Information). Circular nanosheets consisting of PLGA and MNPs were micropatterned on either glass or SiO_2 substrates (**Figure 1**a). The shape or diameter of the micropatterned nanosheets could be varied from 300 to 1000 μm by adjusting the microstructure of the PDMS mold (Figure S2, Supporting Information). Dissolution of the PVA sacrificial layer allowed the release of the brown-colored nanosheets (Figure 1b, 500 μm ϕ). Surface profilometer measurement showed that the thickness of the micropatterned nanosheets gradually increased toward the center; the mean thickness was ca. 170 nm regardless of MNP incorporation (Figure S3, Supporting Information). The micropatterned nanosheets could be aspirated and injected through a syringe needle or an intravenous catheter due to their highly flexible structure (Movie S1, Supporting Information). Despite the incorporation of MNPs, the micropatterned nanosheets (1000 μm ϕ) were capable of deforming flexibly inside a 24 G catheter needle (470 μm inner diameter) (Figure 1c), as determined by optical and fluorescent imaging (dual-colored by the MNPs and rhodamine B), and could bend along the inner wall of the needle (Figure 1d). In our previous study, we reported that the elastic modulus of polylactide-based nanosheets was less than 5 GPa, which is lower than that of bulk polylactide materials (7–10 GPa).[11] Thus, the micropatterned PLGA nanosheets showed good flexibility and were capable of bending inside a needle without distortion or crease formation. In fact, such flexible property has a significant advantage in cell delivery, since conventional substrates consisting of synthetic polymers are relatively bulk and rigid;[5] thus, a large incision to the sclera is required for the subretinal transplantation of the synthetic substrates. The injection of micropatterned nanosheets through a syringe needle could be a minimal invasive way to reduce the incision size of the sclera and subsequent inflammatory response. It is also noteworthy that we succeeded in the preparation of nanosheets with different morphologies by applying microfabrication technique such as circles, triangles and stars by arranging the design of PDMS molds (Figure S4, Supporting Information). The morphological variation of the micropatterned nanosheets would be beneficial for arrangement of the shape of the nanosheet, depending on the physical configuration of the transplantation site.

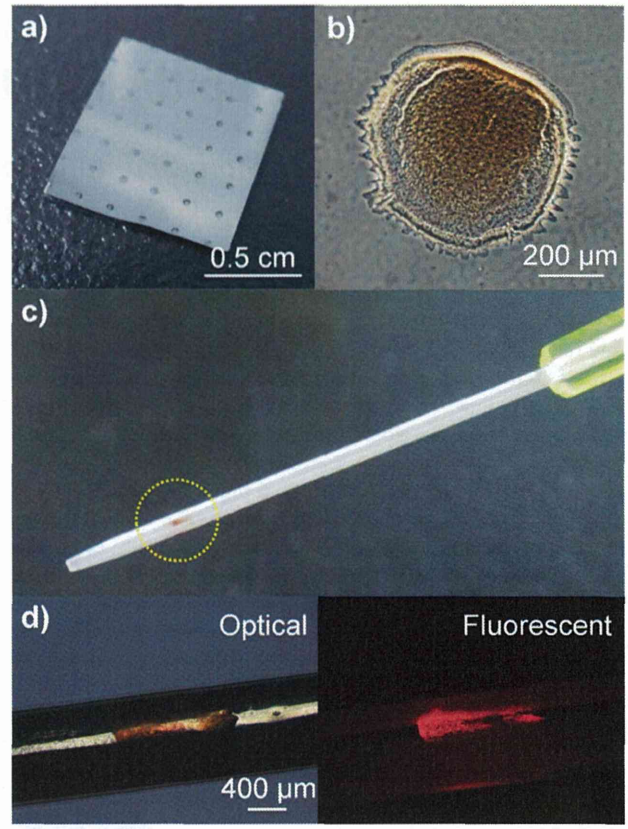

Figure 1. Typical morphology of micropatterned nanosheets. a) Macroscopic image of micropatterned nanosheets. b) Microscopic image of a single micropatterned nanosheet colored brown by the inclusion of MNPs (ϕ 500 μm). c) A micropatterned nanosheet (ϕ 1000 μm) aspirated into a 24 G intravenous catheter (470 μm inner diameter). d) Higher magnification images of the nanosheet in (c) showing that it forms a flexibly deformed structure along the inner wall of the needle.

Next, we cultured RPE-J cells on micropatterned nanosheets. We prepared the micropatterned nanosheets on PVA-coated glass substrates. Prior to seeding the cells, the surface was covered with collagen by spincoating to promote cell adhesion. Phase microscopy analysis following staining for live/dead

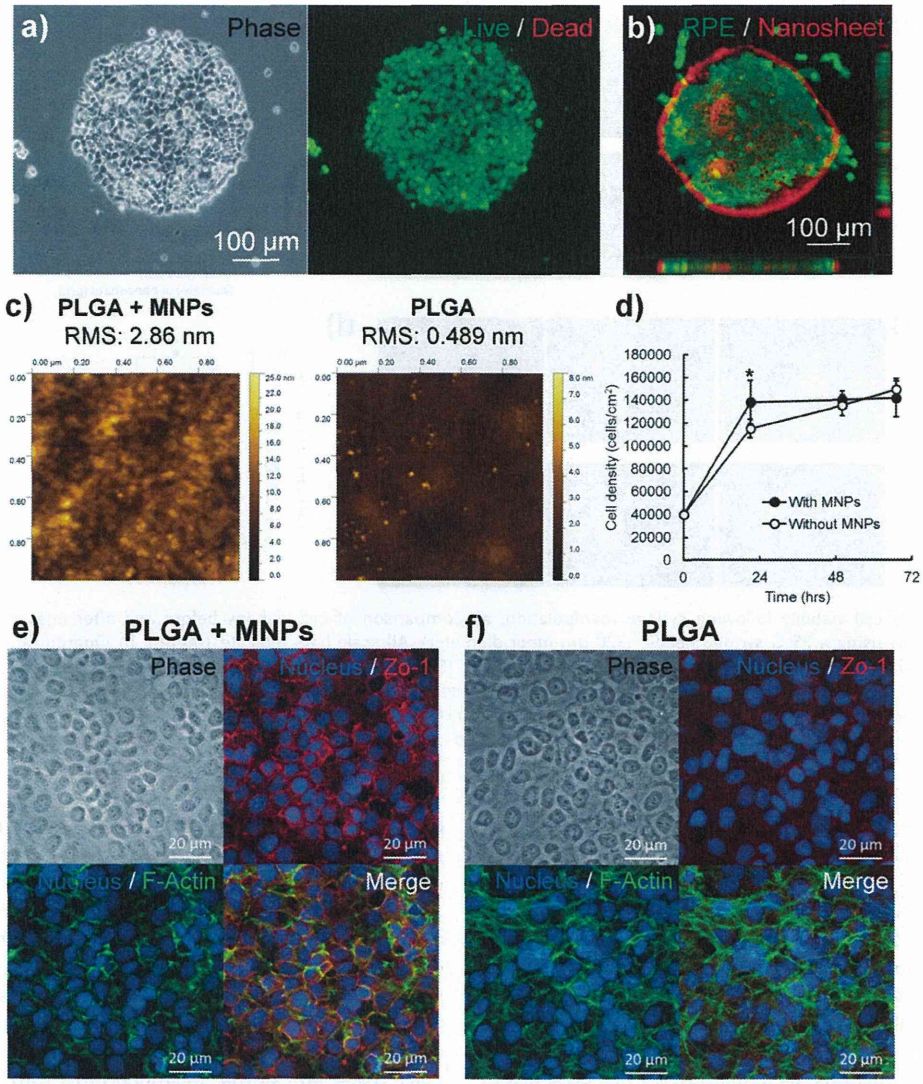

Figure 2. Micropatterned nanosheets direct RPE-J cellular morphogenesis. a) RPE-J cells on micropatterned nanosheets (400 μm ϕ) after 1 d of culture stained to show live/dead cells. b) A CLSM image showing monolayer formation by the RPE-J cells on the nanosheet (stained with rhodamine B). c) AFM surface morphology of micropatterned PLGA nanosheets with and without MNPs. d) Influence of MNPs on the proliferation of RPE-J cells. Immunostaining of the RPE monolayer on the nanosheet e) with and f) without MNPs (top left, phase microscopy; top right, nucleus and tight junction protein ZO-1; bottom left, nucleus and F-actin; bottom right, merged image). On the MNP surface, the RPE-J cells showed bridges among the ZO-1 tight junctions with hexagonal structures. Student *t*-test with $*p < 0.05$ set as the level of statistical significance.

cells showed that the RPE-J cells adhered to the micropatterned nanosheet and remained viable; no adherent cells were observed outside the nanosheet due to the swelling of the PVA layer (**Figure 2**a). We then analyzed cellular organization using a confocal laser scanning microscope (CLSM) to determine whether the RPE-J cells formed a monolayer. CLSM images clearly showed monolayer formation by the RPE-J cells (colored green by calcein AM) on the micropatterned nanosheet (colored red by rhodamine B) (Figure 2b). Also, the rim of the nanosheet (see Figure S3, Supporting Information) was clearly observed in the CLSM image. The RPE monolayer formed consistently across the nanosheet, as confirmed by cross-sectional images. In addition to monolayer formation, RPE cells formed a densely packed structure (a "cobblestone-like" morphology) that is critical for their ability to function as a barrier under physiological conditions.[12] It has been reported that the nanostructured surface generated by nanoparticles or by means of electron beam lithography has a significant impact on cell proliferation or cytoskeletal organization at the nanoscale.[13] Thus, we sought to influence RPE cell morphogenesis by modulating the surface structure of the nanosheets with MNPs. Atomic force microscope (AFM) measurements revealed that the inclusion of MNPs generated a rough surface (Figure 2c); the surface roughness (root-mean-squared value) was increased by more than 5 times by the inclusion of MNPs from 0.489 nm ([MNPs] = 0 mg mL^{-1}) to 2.86 nm ([MNPs] = 2.5 mg mL^{-1}).

ADVANCED MATERIALS
www.advmat.de

Materials Views
www.MaterialsViews.com

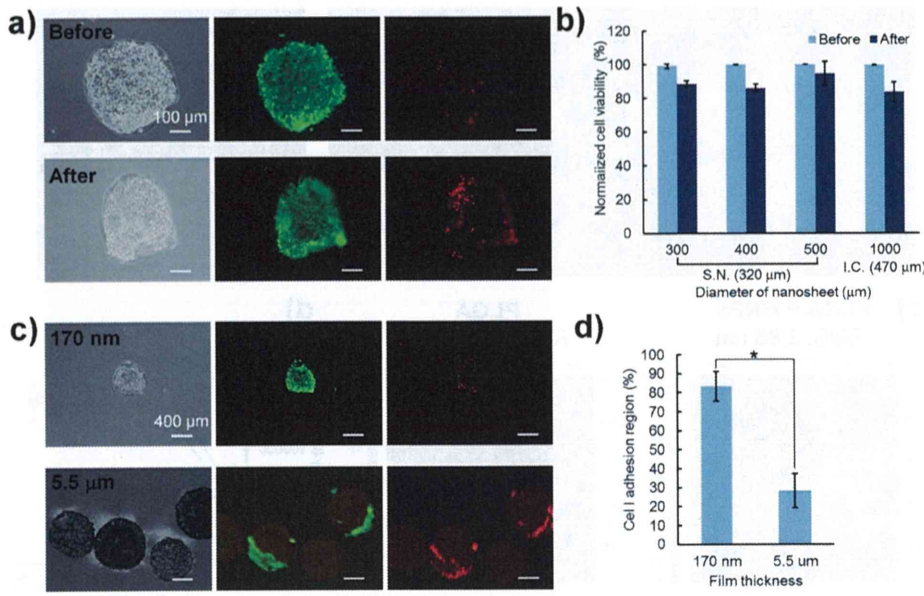

Figure 3. Evaluation of cell viability following syringe manipulation. a) Comparison of cell viability before and after injection of micropatterned nanosheets (400 μm ϕ) using a 25 G syringe needle (320 μm inner diameter). All scale bars indicate 100 μm. b) Quantification of cell viability on micropatterned nanosheets of different diameters. A 25 G syringe needle (S.N.) was used for nanosheets of 300 to 500 μm diameter, and a 24 G intravenous catheter (I.C.) was used for nanosheets of 1000 μm (the diameter of each needle is indicated below the Figure). c) Mechanical stability of cellular organization on micropatterned nanosheets (400 μm ϕ) of 170 nm or 5.5 μm thickness (all scale bars indicate 400 μm). d) Quantification of the cell adhesion region after syringe manipulation. Student's *t*-test with $^*p < 0.05$ set as the level of statistical significance.

This level of increase in roughness is consistent with that found in our previous study using polylactide nanosheets modified by MNPs.[10a] We compared the proliferation of RPE-J cells on nanosheets with and without MNPs and found that a significantly enhanced rate of proliferation occurred after 1 d of culture on the surface with MNPs (Figure 2d, $p < 0.05$). Immunohistochemical analysis of the morphogenesis in the RPE monolayer after 2 d of culture showed that cells on the surface with MNPs had a hexagonal structure with abundant formation of tight junctions, as visualized by the presence of the tight junction protein ZO-1 (Figure 2e); by contrast, cells on surfaces without MNPs were randomly organized (Figure 2f). Stress fibers (F-actin) formed along the tight junctions in cells on the surface with MNPs, but were less organized on cells on surfaces without MNPs. After 7 d of culture, the formation of tight junctions had occurred on both surfaces (data not shown). A previous study reported that cells grown on a nanoparticle-modified surface showed an increased area of contiguous contact of the cell membrane (endothelial cells) with the underlying substrate, and also showed a consistent increase in growth of F-actin filaments.[13a] Therefore, we anticipated that the greater surface roughness generated by MNPs would enhance cell migration and proliferation, and result in faster maturation of tight junctions in the epithelial monolayer. With regard to use of RPE cells in clinical applications, such enhanced morphogenesis on a micropatterned nanosheet would accelerate the process of transplantation of RPE monolayers.

On the assumption that transplantation of engineered RPE monolayers would be carried out using conventional syringe needles, we evaluated cell viability following mechanical compression of the micropatterned nanosheets inside a syringe needle that had a circular opening. The stability and viability of the RPE monolayer was evaluated on micropatterned nanosheets with different diameters by analyzing the cells after live/dead staining. After 2 d of culture, the cell/nanosheet constructs were detached from the glass substrate by gently scratching and rubbing the corner of the nanosheets. Due to the magnetic properties of the nanosheets, the freely suspended cell–nanosheet constructs could be remotely gathered in one place using an external magnetic force (Movie S2, Supporting Information); this enabled a minimally invasive collection of the engineered RPE monolayer. Each construct was then aspirated and injected through a 25 G syringe needle (320 μm inner diameter) at 10 mL min^{-1}. Despite the mechanical stress during syringe manipulation, the RPE monolayer retained its original shape without distortion (**Figure 3**a). Following cell staining, we estimated a rate of cell viability of over 80% for nanosheets ranging in diameter from 300 to 500 μm (Figure 3b). The ratio of the diameter of the nanosheet to that of the syringe needle was crucial for minimizing cell mortality during the manipulation process. If the inner diameter was increased, as in switching from a 25 G syringe needle (320 μm) to a 24 G intravenous catheter (470 μm), a micropatterned nanosheet of 1000 μm diameter could be injected without significant loss of cell viability (more than 85%) (see also Figure S5). These results suggest that the micropatterned nanosheet can withstand deformation in syringe needles with an internal diameter up to half that of the nanosheet. Furthermore, we also evaluated the effect of the thickness of the nanosheet on cell viability following syringe manipulation. Micropatterned nanosheets with

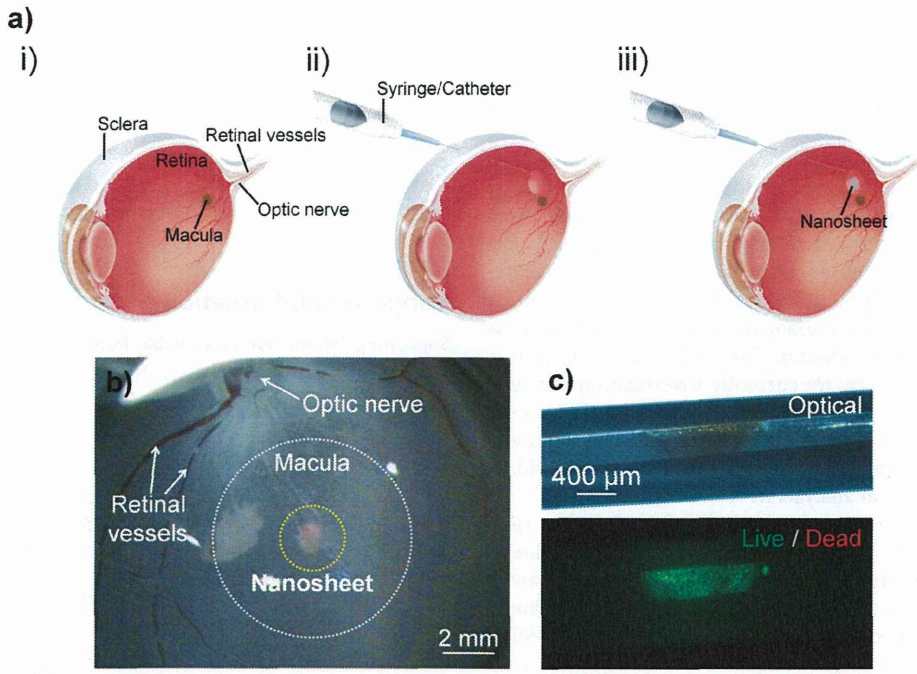

Figure 4. Injection of a micropatterned nanosheet into the subretinal space of a swine eye ex vivo. a) Schematic representation of the injection process: i) fresh swine eyeball without the detachment of retinal tissue, ii) subretinal injection of saline to make a space for injection, and, iii) injection of the micropatterned nanosheet (1000 μm ϕ) using a 24 G intravenous catheter (470 μm in inner diameter). b) Microscopic image of the injected nanosheet (stained with rhodamine B), which was fixed on the macula after removal of the saline. c) Staining of the micropatterned nanosheet with RPE-J cells in the catheter to show live/dead cells.

thicknesses of a few hundred of nanometers (170 nm) retained viable cells on the surface, whereas those that were micrometers in thickness (5.5 μm) retained few cells, with most showing low viability (Figure 3c). We assumed that cells on the latter nanosheets had been scraped from the surface during manipulation, resulting in only a few cells remaining. Such phenomena would be explained from the feasible elastic properties between cells and the 170 nm-thickness nanosheets rather than the 5.5 μm-thickness sheets; the more flexible substrate could retain the cellular organization under the mechanical stress. Indeed, comparison of the sizes of the cell adhesion regions showed that the thicker nanosheets had a significantly reduced area (Figure 3d). Overall, therefore our findings show that the ultrathin flexible structure of the micropatterned nanosheets is beneficial for aspirating them into a narrow space, such as a syringe needle, and also reduces the mechanical stress on the attached cells.

Finally, we used our system to deliver micropatterned nanosheets to the subretinal space of a swine eye ex vivo. Before injection of the nanosheet, the subretinal space was partially filled with saline in order to secure the transplanted site (**Figure 4**a). As the macula of the swine ocular ball is large, we injected a 1000 μm ϕ micropatterned nanosheet using a 24 G intravenous catheter. The nanosheet was successfully injected and spread into the subretinal space (see Movie S3, Supporting Information); it then attached to the macula and retained its circular shape after removal of the saline (Figure 4b). In addition, staining for live/dead cells showed that the RPE monolayer was stable inside the catheter needle and retained cellular activity (Figure 4c). Thus, the ex vivo results confirm the practicality of using micropatterned nanosheets for delivering an RPE monolayer in a therapeutic context. In this ex vivo study, the fixation of the cell monolayer after injection was facilitated by removal of the prefilled saline, since the native RPE layer is closely sandwiched between the retinal photoreceptors and the choroid. Thus, removal of the saline would be sufficient to fix the transplanted RPE monolayer stably. In addition, the number of cells on the nanosheet is basically adjustable in line with the AMD size. Therefore, it may be possible to inject multiple nanosheets through the syringe needle unless the prefilled saline is removed from the subretinal place. Such multiple injections would enhance the transplantation efficacy.

It was previously reported that polylactide nanosheets from 20 to 200 nm thick degraded within 1 week under physiological enzymatic conditions and also showed minimal inflammatory response in vivo due to the small amount of polymer.[14] For further estimation, we are currently investigating the biodegradability of the micropatterned nanosheets by using model eye fluid, such as aqueous humor (data not shown). In addition, it has recently been reported that MNP-labeled cells can be transplanted into rat retina without inducing a significant inflammatory response.[15] Thus, we incorporated MNPs or fluorescent dyes into the micropatterned nanosheets in order to visualize the structure, improve the ease of manipulation, and enhance cellular morphogenesis. Moreover, these materials can be substituted by other chemicals. For example,

fluorescein can be used as a dye since it is clinically available. The roughness effect induced by MNP could also be recapitulated by integrating microfabricated structure in the nanosheet (e.g., micropores or nano/microcues). Similar techniques could also be used to incorporate the drugs necessary for further improving the function of the nanosheet, that will be applied for drug delivery system.[16] For example, it may be possible to enhance the tissue integration of the transplanted RPE monolayer through the controlled release of drugs and growth factors from the micropatterned nanosheet. Thus, the micropatterned nanosheet will not only be of value for retaining cellular organization but also for enhancing cellular activity such as proliferation and differentiation. For further characterization of the tissue function, we are currently investigating transepithelial electrical resistance (TER) of the engineered RPE monolayer on the nanosheet using a volt–ohm meter.[13b] In addition, integration of the engineered tissue to the host tissue will be examined by histological analysis in vivo.

With respect to the clinical treatment of AMD using stem cells, such as induced pluripotent stem (iPS) cells,[17] it should be noted that the present technique for directing transplanted cells using micropatterned nanosheets may also be applicable for differentiated RPE cells from stem cells providing they adhere to the nanosheet. In particular, transplanted cells might induce apoptosis unless they attach correctly to the basement membrane;[18] the rate of attachment may depend on the anatomy and physiology of the basement membrane. In this regard, a micropatterned nanosheet may offer a good microenvironment for transplanted cells since the high flexibility of the nanosheet permits the stable attachment of the RPE monolayer despite the complicated surface of the retinal lesion. In addition, conventional cell-sheet engineering has to wait for cell confluence in order to detach the cells as a freestanding structure.[19] To this end, the nanosheets will provide stable platforms for the cells, on which the organized cells can be detached even without waiting for the cell maturation. Therefore, integration of the nanosheet technology into cell-sheet engineering may reduce the cell culture period and also enhance the overall transplantation process.

In summary, we described the development of micropatterned nanosheets that consisted of biodegradable PLGA and MNPs toward local delivery of RPE cells for the treatment of AMD. The micropatterned nanosheets promoted the formation of a stable monolayer of the RPE-J cells that could differentiate into a cobblestone-like structure. Owing to the high flexibility of the nanosheet, the RPE monolayer could be injected through a clinical syringe without significant loss of cell viability. We also injected micropatterned nanosheets into the subretinal space of a swine eye and showed that they could attach stably to the macula. Our results indicate that micropatterned nanosheets are useful substrates not only for delivery of RPE-J cells but also for enhancing morphogenesis in the cells, such as monolayer formation with hexagonal tight junctions. Furthermore, manipulability by magnetic force would be exploited for the minimally invasive delivery of the engineered RPE-J cells. In order to further improve cell transplantation methods, such as those for iPS cells, development of cell resources as well as effective delivery technique will play an important role for the enhancement of therapeutic efficacy. Flexible micropatterned nanosheets hold great promise for transplantation of organized cellular structures and for the development of local cell delivery systems.

Experimental Section

Experimental details are described in the Supporting Information.

Supporting Information

Supporting Information is available from the Wiley Online Library or from the author.

Acknowledgements

The authors thank Dr. Hao Liu and Prof. Ken Nakajima (WPI-AIMR, Tohoku University) for the AFM analysis. This work was supported by the World Premier International Research Center Initiative (WPI) and JSPS KAKENHI (grant number 25870050 for T.F., and 23681027 and 24651156 for H.K.) from MEXT, Japan, and the 5th Mandom International Research Grants on Alternative to Animal Experiments (H.K.).

Received: August 20, 2013
Revised: September 17, 2013
Published online: December 4, 2013

[1] S. R. Hynes, E. B. Lavik, *Graefes. Arch. Clin. Exp. Ophthalmol.* **2010**, *248*, 763.
[2] S. Binder, B. V. Stanzel, I. Krebs, C. Glittenberg, *Prog. Retin. Eye Res.* **2007**, *26*, 516.
[3] a) T. Abe, M. Yoshida, Y. Yoshioka, R. Wakusawa, Y. Tokita-Ishikawa, H. Seto, M. Tamai, K. Nishida, *Prog. Retin. Eye Res.* **2007**, *26*, 302; b) T. Abe, Y. Saigo, M. Hojo, T. Kano, R. Wakusawa, Y. Tokita, M. Tamai, *Cell Transplant.* **2005**, *14*, 799; c) Y. Saigo, T. Abe, M. Hojo, H. Tomita, E. Sugano, M. Tamai, *Invest. Opthalmol. Vis. Sci.* **2004**, *45*, 1996.
[4] a) A. Khademhosseini, R. Langer, J. Borenstein, J. P. Vacanti, *Proc. Natl. Acad. Sci. USA* **2006**, *103*, 2480; b) A. Khademhosseini, J. P. Vacanti, R. Langer, *Sci. Am.* **2009**, *300*, 64; c) N. E. Vrana, P. Lavalle, M. R. Dokmeci, F. Dehghani, A. M. Ghaemmaghami, A. Khademhosseini, *Tissue Eng. B Rev.* **2013** DOI: 10.1089/ten.teb.2012.0603.
[5] a) G. Thumann, A. Viethen, A. Gaebler, P. Walter, S. Kaempf, S. Johnen, A. K. Salz, *Biomaterials* **2009**, *30*, 287; b) S. Tao, C. Young, S. Redenti, Y. Zhang, H. Klassen, T. Desai, M. J. Young, *Lab Chip* **2007**, *7*, 695; c) B. V. Stanzel, Z. Liu, R. Brinken, N. Braun, F. G. Holz, N. Eter, *Invest. Opthalmol. Vis. Sci.* **2012**, *53*, 490.
[6] J. A. Forrest, K. Dalnoki-Veress, *Adv. Colloid Interface Sci.* **2001**, *94*, 167.
[7] T. Fujie, Y. Okamura, S. Takeoka, in *Functional Polymer Films*, Vol. *2* (Eds: W. Knoll, R. C. Advincula), Wiley-VCH, Weinheim, Germany **2011**, p. 907.
[8] a) T. Fujie, Y. Okamura, S. Takeoka, *Adv. Mater.* **2007**, *19*, 3549; b) T. Fujie, N. Matsutani, M. Kinoshita, Y. Okamura, A. Saito, S. Takeoka, *Adv. Funct. Mater.* **2009**, *19*, 2560; c) T. Fujie, S. Furutate, D. Niwa, S. Takeoka, *Soft Matter* **2010**, *6*, 4672.
[9] a) T. Fujie, L. Ricotti, A. Desii, A. Menciassi, P. Dario, V. Mattoli, *Langmuir* **2011**, *27*, 13173; b) T. Fujie, A. Desii, L. Ventrelli, B. Mazzolai, V. Mattoli, *Biomed. Microdevices* **2012**, *14*, 1069.

[10] a) S. Taccola, A. Desii, V. Pensabene, T. Fujie, A. Saito, S. Takeoka, P. Dario, A. Menciassi, V. Mattoli, *Langmuir* **2011**, *27*, 5589; b) T. Fujie, S. Ahadian, H. Liu, H. Chang, S. Ostrovidov, H. Wu, H. Bae, K. Nakajima, H. Kaji, A. Khademhosseini, *Nano Lett.* **2013**, *13*, 3185.

[11] a) T. Fujie, Y. Kawamoto, H. Haniuda, A. Saito, K. Kabata, Y. Honda, E. Ohmori, T. Asahi, S. Takeoka, *Macromolecules* **2013**, *46*, 395; b) B. Eling, S. Gogolewski, A. J. Pennings, *Polymer* **1982**, *23*, 1587.

[12] a) A. R. Harris, L. Peter, J. Bellis, B. Baum, A. J. Kabla, G. T. Charras, *Proc. Natl. Acad. Sci. USA* **2012**, *109*, 16449; b) C. Guillot, T. Lecuit, *Science* **2013**, *340*, 1185.

[13] a) A. M. Lipski, C. J. Pino, F. R. Haselton, I. W. Chen, V. P. Shastri, *Biomaterials* **2008**, *29*, 3836; b) K. R. Kam, L. A. Walsh, S. M. Bock, M. Koval, K. E. Fischer, R. F. Ross, T. A. Desai, *Nano Lett.* **2013**, *13*, 164.

[14] a) Y. Okamura, K. Kabata, M. Kinoshita, D. Saitoh, S. Takeoka, *Adv. Mater.* **2009**, *21*, 4388; b) K. Fujino, M. Kinoshita, A. Saitoh, H. Yano, K. Nishikawa, T. Fujie, K. Iwaya, M. Kakihara, S. Takeoka, D. Saitoh, Y. Tanaka, *Surg. Endosc.* **2011**, *25*, 3428; c) Y. Okamura, K. Kabata, M. Kinoshita, H. Miyazaki, A. Saito, T. Fujie, S. Ohtsubo, D. Saitoh, S. Takeoka, *Adv. Mater.* **2013**, *25*, 545.

[15] A. Yanai, U. O. Häfeli, A. L. Metcalfe, P. Soema, L. Addo, C. Y. Gregory-Evans, K. Po, X. Shan, O. L. Moritz, K. Gregory-Evans, *Cell Transplant.* **2012**, *21*, 1137.

[16] a) T. Fujie, A. Saito, M. Kinoshita, H. Miyazaki, S. Ohtsubo, D. Saitoh, S. Takeoka, *Biomaterials* **2010**, *31*, 6269; b) A. Saito, H. Miyazaki, T, Fujie, S. Ohtsubo, M. Kinoshita, D. Saitoh, S. Takeoka, *Acta Biomater.* **2012**, *8*, 2932; c) K. Kashiwagi, K. Ito, H. Haniuda, S. Ohtsubo, S. Takeoka, *Invest. Opthalmol. Vis. Sci.* **2013**, *54*, 5629.

[17] a) K. Takahashi, S. Yamanaka, *Cell* **2006**, *126*, 663; b) T. Kuroda, S. Yasuda, S. Kusakawa, N. Hirata, Y. Kanda, K. Suzuki, M. Takahashi, S. Nishikawa, S. Kawamata, Y. Sato, *PLoS One* **2012**, *7*, e37342; c) D. Cyranoski, *Nature* **2013**, *494*, 413.

[18] a) L. V. Del Priore, T. H. Tezel, *Arch. Ophthalmol.* **1998**, *116*, 335; b) T. H. Tezel, L. V. Del Priore, *Invest. Ophthalmol. Vis. Sci.* **1999**, *40*, 767.

[19] a) N. Matsuda, T. Shimizu, M. Yamato, T. Okano, *Adv. Mater.* **2007**, *19*, 3089; b) H. Takahashi, M. Nakayama, M. Yamato, T. Okano, *Biomacromolecules* **2010**, *11*, 1991.